

# Weak-Field Femtosecond Coherent Control of Thermally-Hot Unbound Collision Pair is Feasible

Moran Geva,<sup>1</sup> Yonathan Langbeheim,<sup>1</sup> Arie Landau,<sup>2</sup> and Zohar Amitay<sup>1,\*</sup>

<sup>1</sup>*The Shirlee Jacobs Femtosecond Laser Research Laboratory,*

*Schulich Faculty of Chemistry, Technion-Israel Institute of Technology, Haifa 32000, Israel*

<sup>2</sup>*Institute of Advanced Studies in Theoretical Chemistry and Schulich Faculty of Chemistry,  
Technion-Israel Institute of Technology, Haifa 32000, Israel*

(Dated: January 18, 2023)

Femtosecond coherent control of a thermally-hot unbound collision pair is crucial for the yet unrealized coherent control of binary photo-reactions. We experimentally demonstrate here its feasibility in the important weak-field regime. Linearly chirped pulses control the photo-excitation yield of a thermally-hot ensemble of unbound K-Ar collision pairs, which are excited at short internuclear distances via a molecular (KAr) weak-field resonance-mediated two-photon absorption. Enhancement by negative chirps is observed. Our *ab initio* theoretical studies support and explain the experiments. The control mechanism combines two-step Franck-Condon filtering and chirp-dependent resonance-mediated excitation of the filtered excitation channels.

PACS numbers: 42.65.Re, 82.50.Nd, 82.50.Pt, 82.53.Eb, 82.53.Kp

One of the holy grails in the field of quantum coherent control is the yet-to-be-realized coherent control of photo-induced thermal binary reactions [1–4]. The operating principle is to use shaped femtosecond pulses [5] to control and actively drive binary chemical reaction along its full desired path from the thermal initial state of the reactants to the final state of the desired products. This is actually one of the dreams that led, more than thirty years ago, to the birth of the coherent control concept. Its realization will enable a novel type of photochemistry that is conceptually different from the common photochemistry, where photo-excited reactants react under no irradiation. The first part of the control scheme is a controlled ultrafast photo-excitation of the thermal unbound collision pair of reactants that takes place at short internuclear distances. It generates the system in an excited electronic molecular state with the nuclear wave-function localized at these short distances. This generated quantum state generally involves both bound and unbound molecular eigenstates, with populations and coherences among them. It then serves as a launch state for further photo-control toward the desired products, with controlled branching ratios and yields.

For long, such ultrafast coherent control of a thermal unbound collision pair has been considered unfeasible, particularly when the corresponding temperatures are hundreds of degrees ("thermally-hot collision pair"). The main unique challenges are the initial close-to-zero quantum purity and the very low excitation yields per pulse. The former is fundamental from both a theoretical and an experimental point of view, while the latter is an applicative experimental one. They both originate from the nature of the initial thermal state of the system in which an extremely large number of free eigenstates is populated. However, in recent years, the feasibility has been demonstrated and established

in the strong-field excitation regime with thermally-hot unbound atomic collision pair [6–10]. In these studies, strong-field coherent control using shaped femtosecond pulses has been demonstrated experimentally and theoretically over the photo-excitation of a collision pair of thermally-hot magnesium atoms. The corresponding excitation has involved non-resonant two-photon free-to-bound transitions into strongly-bound molecular states of Mg<sub>2</sub> and subsequent bound-bound transitions, photo-driving the excited molecule into different target states. In this Letter, we extend this significant strong-field feasibility to the important weak-field regime, demonstrating weak-field femtosecond coherent control of thermally-hot collision pair with linearly chirped pulses. The experiments are supported by first-principles theoretical studies. This establishes another important milestone toward chemical reaction control.

Since its introduction more than twenty years ago, weak-field femtosecond coherent control [11–30] has extensively been very powerful and successful, both conceptually and practically, in controlling few-photon excitations of initially-bound systems. The weak-field excitation regime refers to the intensity regime where the photo-excitation can be fully described within the corresponding lowest-order time-dependent perturbation theory. For example, for a weak two-photon excitation, it is the second-order one. This is in contrast to the strong-field regime, where no perturbative description is valid and a full non-perturbative time-dependent analysis is required. The valid time-dependent perturbative description of the weak-field regime is very powerful for coherent control since its transformation to the frequency domain allows to fully identify the initial-to-final multiphoton excitation pathways of the system and understand the coherent interference mechanism among them. The pulse spectral intensity determines the manifold of excitation

pathways with their relative amplitudes, while the pulse spectral phase sets their relative phases. As indicated, the success of weak-field femtosecond coherent control has been experimentally limited so far only to physical systems that are bound in their initial state. The present work is first also in terms of demonstrating weak-field femtosecond control with an initially-unbound system.

The benchmark system of the present study is the heteronuclear K-Ar system. Figure 1 shows the present excitation scheme with the relevant molecular electronic states and transition dipole moments of KAr. Initially, a thermally-hot ensemble of K and Ar atoms is held at a temperature of  $T = 573$  K ( $\kappa_B T \approx 400$  cm $^{-1}$ ). The electronic ground state  $X^2\Sigma^+$  has a van der Waals nature with a very shallow rotationless potential well of only  $\sim 40$  cm $^{-1}$ , and with the rotational-barrier addition it does not support any bound levels for all the partial waves above  $J \approx 40$  ( $J$  is the rotational quantum number). So, at the present hot temperature, the initial thermal population of the  $X^2\Sigma^+$  state predominantly occupies (unbound) scattering eigenstates. Following their little initial thermal population, in combination with their very low relative excitation probability (see below), the bound eigenstates of  $X^2\Sigma^+$  play here a negligible role.

In the scheme, following the ensemble irradiation with a phase-shaped femtosecond pulse, collision pairs of K and Ar atoms populating these scattering states are photo-excited at short internuclear distances in a molecular weak-field resonance-mediated two-photon absorption from the  $X^2\Sigma^+$  state via the  $A^2\Pi$  and  $B^2\Sigma^+$  states to the  $(3)^2\Pi$  and  $(5)^2\Sigma^+$  states. Following the initial thermal population distribution, the short internuclear distances relevant for the X–A and X–B transitions are those above  $R \sim 3.0$  Å. At these distances, the X–A potential-energy curves difference (PECD) matches the full spectrum of the present exciting pulse, with the corresponding Franck-Condon window (FCW) located at  $R \sim 3.4$ – $3.7$  Å, while the X–B PECD is far detuned from the spectrum. Then, with the A-state, the A– $(5)^2\Sigma^+$  PECD matches the low-frequency edge of the spectrum, having the corresponding FCW located at  $R \sim 3.2$ – $3.4$  Å, while the A– $(3)^2\Pi$  one is also far detuned from the spectrum. Hence, the dominant excitation channel in terms of end population is the  $X^2\Sigma^+ - A^2\Pi - (5)^2\Sigma^+$  channel. This conclusion is also supported by the full theoretical results. For convenience, in all the following we will consider only this dominant channel. Following the broad spectrum of the pulse, the excitation from each of the initial unbound eigenstates in the  $X^2\Sigma^+$  state coherently goes through multiple intermediate eigenstates in the  $A^2\Pi$  state, and ends up at multiple final eigenstates in the  $(5)^2\Sigma^+$  state. Both bound and unbound eigenstates are involved in the excitation as intermediates and finals. As mentioned, the end population excited from bound eigenstates in  $X^2\Sigma^+$  is negligible due to their small initial population and very low excitation probability. The latter results from the

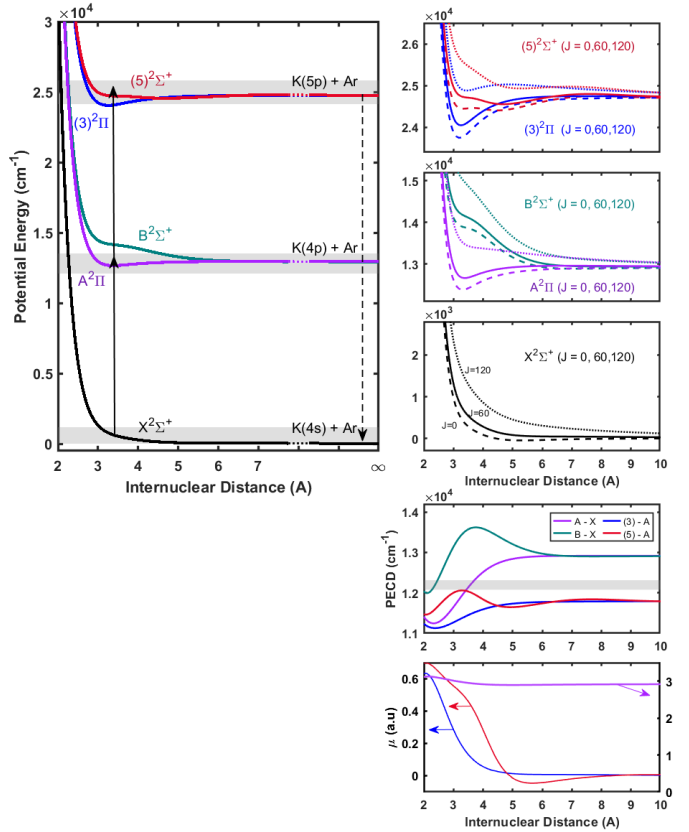


FIG. 1: The excitation of a thermally-hot unbound K-Ar collision pair via weak-field femtosecond resonance-mediated two-photon absorption and the relevant potential energy curves of KAr. All the potentials are weakly bound or completely unbound, depending on the rotational quantum number  $J$ . Examples are shown in the right panels for  $J=0$  (dashed lines), 60 (solid lines) and 120 (dotted lines). The left panel corresponds to  $J=60$ . The shaded areas on the potentials show the thermally populated X-state scattering states and the bands of excited states energetically accessible via the excitation. Also shown are relevant differences (PECDs) and electronic transition dipole moments ( $\mu$ ) between potentials. The shaded area on the PECDs shows the range of the exciting pulse spectrum.

fact that their present excitation is non-resonant with the  $A^2\Pi$  state. This negligible contribution is also obtained in the full theoretical results. Similar to the X-state, also the  $A^2\Pi$  and  $(5)^2\Sigma^+$  states are weakly bound or completely unbound, depending on  $J$ . Their rotationless well depths are of about 500 and 300 cm $^{-1}$  and their bound levels exist only up to  $J \approx 90$  and 80, respectively.

The KAr molecules generated at the  $(5)^2\Sigma^+$  state have their vibrational (radial) wave-function localized at short internuclear distances. After the pulse excitation, they are detected upon their dissociation to the atomic fragments K(5p) and Ar( $^1S$ ) at the state's asymptote, and the subsequent spontaneous decay of the former via the  $5p \rightarrow 4s$  emitting transition. There is no other source here

for excited K(5p) atoms, since the atomic two-photon transition between ground-state K(4s) and excited K(5p) is forbidden and also, accordingly, the  $A^2\Pi-(5)^2\Sigma^+$  KAr molecular electronic transition dipole moment is practically zero at distances beyond 10 Å (see Fig. 1). So, this  $5p \rightarrow 4s$  emission intensity is a background-free measure for the generated molecular yield of our interest.

The exciting femtosecond pulse has a linear polarization, central wavelength of 820 nm, a spectral bandwidth of  $\sim 120 \text{ cm}^{-1}$  ( $\sim 8.1 \text{ nm}$ ), a transform-limited (TL) duration of 125 fs, and TL peak intensity of  $5 \times 10^{10} \text{ W/cm}^2$ . The spectral phase of the linearly-chirped pulses is of the form  $\Phi(\omega) = \frac{1}{2}k(\omega - \omega_0)^2$ , with  $\omega_0$  the central frequency and  $k$  the linear chirp parameter. The unchirped, or TL, pulse corresponds to  $k=0$ . The chirp parameter is the present control variable.

The experiments take place in a static cell at 573 K holding a gas mixture of potassium and argon, with the K vapor pressure being about 0.3 Torr and the Ar pressure set to 60 Torr. The sample is irradiated at 1-kHz repetition rate by the linearly chirped femtosecond pulses, after they undergo shaping in a setup incorporating a liquid-crystal spatial light phase modulator [5]. The spontaneously-emitted radiation is optically collected and then detected by a spectrometer and a time-gated camera system. The integrated intensity of the  $5p \rightarrow 4s$  emission line of K at  $\sim 404.5 \text{ nm}$ ,  $I_{5p}$ , is measured as a function of the applied chirp.

As described, the emitting K(5p) atoms are generated via the dissociation of the KAr molecules generated in the  $(5)^2\Sigma^+$  state. Due to the experimental conditions, they include not only all these molecules generated as unbound (which naturally dissociate), but also those generated as bound. The bound ones dissociate upon their collisions with the Ar atoms. Based on experiments with other similar systems [31], we estimate the present Ar-induced collisional dissociation lifetime of different  $(5)^2\Sigma^+$ 's bound levels to be shorter than 5 ns. Such collisional dissociation dominants over the other bound-level decay possibility of spontaneous emission, for which we have calculated a much longer lifetime of about 120–150 ns. This radiative lifetime value is consistent with the  $\sim 135$ -ns value measured for K(5p) [32–34].

Regarding the  $I_{5p}$  measurements, the measured chirp dependence of  $I_{5p}$  is independent on the TL peak intensity, as expected for a weak-field process. For a given pulse, the  $I_{5p}$  signal exhibits linear dependence on the K and Ar partial pressures, as expected for an excitation of K-Ar pairs, and quadratic dependence on the TL peak intensity, as expected in the weak-field regime for a two-photon process. As no atomic excitation of ground-state K(4s) can produce here K(5p) atoms, no signal is indeed measured with only K vapor in the cell. Another observation is that blocking the pulse spectrum at wavelengths shorter than 813 nm does not affect the measured  $I_{5p}$  and its chirp dependence. Such blocking disables any

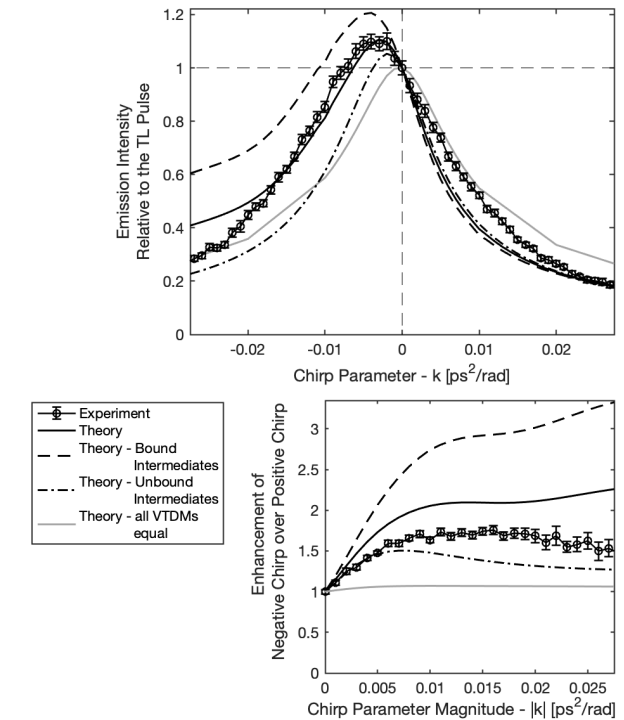


FIG. 2: Experimental and theoretical chirp-dependent results for the emission intensity signal  $I_{5p}$ . (a) Enhancement by a linearly-chirped pulse relative to the TL pulse. (b) Enhancement by a negatively-chirped pulse relative to the positively-chirped pulse of the same chirp magnitude. The theoretical results include the full results (solid lines) as well as results for several case of specific analysis. See text for details.

two-photon transitions having a total wavelength shorter than 406.5 nm, including the  $4s \rightarrow 5p$  two-photon transition of K at  $\sim 404.5 \text{ nm}$ . So, also this observation is consistent with no K(5p) being produced here via two-photon excitation of K(4s).

The experimental results demonstrating weak-field coherent control of thermally-hot collision pair are presented in Fig. 2. Figure 2(a) presents the measured emission intensity  $I_{5p}$ , normalized with respect to the one obtained for the TL pulse, versus the chirp parameter  $k$ . The presented quantity is thus the enhancement factor  $\text{EF}(k) = I_{5p}(k)/I_{5p}(k=0)$ . Several main features are observed for the chirp control. One feature is the enhancement that negatively chirped pulses with small chirps exhibit over the TL pulse. The maximal EF of  $\sim 1.10$  is observed for chirps in the range of  $-0.002$  to  $-0.005 \text{ ps}^2/\text{rad}$ . Another feature is the enhancement that a negatively chirped pulse exhibits over the positively chirped pulse of the same chirp magnitude. The corresponding enhancement by negative chirps,  $\text{EF}_{N/P}(|k|) = I_{5p}(-|k|)/I_{5p}(+|k|)$ , is presented in Fig. 2(b) versus the chirp parameter magnitude ( $|k|$ ). It is higher than 1.50 for all the present magnitudes above  $0.005 \text{ ps}^2/\text{rad}$ , with a weak chirp dependence, and

reaches  $\sim 1.75$  within the range of  $|k| \approx 0.01-0.02 \text{ ps}^2/\text{rad}$ . The degree of coherent control exhibited here is best reflected by  $\text{EF}_{N/P}$  since it corresponds to a pure phase effect, as the two corresponding chirped pulses have identical intensity but different phase in both the time and frequency domains. In terms of the general chirp-dependence trend, for the negative chirps below the chirps of maximal EF, the EF continuously decreases as the negative-chirp magnitude increases. For the positive chirps, this behavior applies over the full range.

To explain the experimental results, our theoretical studies include two sections. The first theoretical part includes state-of-the-art *ab initio* electronic structure calculations of the KAr potential energy curves (PECs) and electronic transition dipole moments (ETDMs). The calculations are performed using the non-relativistic (without spin-orbit coupling) quantum-chemistry package Q-Chem [35]. We employ the equation-of-motion coupled-cluster method restricted to single and double excitations (EOM-CCSD) with the aug-cc-p-3 basis set and frozen core. This basis set yields converged results with respect to the depth of the potential wells and to the asymptotic-atomic transition energies. The convergence has been examined by increasing the principal quantum number of the basis set as well as with respect to experiments. The computation high accuracy is confirmed by the good agreement of the calculated spectroscopic constants with available experimental values for the X, A and B states. The present *ab initio* results of the extended manifold of potentials are much more accurate than previous corresponding results [36, 37]. The full set of the ETDMs is calculated here for the first time. The results of this first part are those presented in Fig. 1. The second theoretical part employs numerical calculations of the shaped femtosecond excitation according to the perturbative frequency-domain formulation presented below. It uses the first part's results for obtaining the bound and unbound eigenstates of the different electronic states (considering also the rotational barrier) and the different vibrationally-averaged transition dipole moments (VTDMs). The eigenstates are numerically calculated using a computational box with a radius of  $120 \text{ \AA}$ . The calculations consider both the vibrational and rotational degrees of freedom.

As noted, the entire controlled excitation of the thermally-hot K-Ar collision pair is composed of a thermal mixture of many separate excitation channels that simultaneously occur and incoherently contribute to the end populations. Each excitation channel corresponds to a coherent weak-field resonance-mediated two-photon femtosecond absorption from one of the thermally-populated unbound eigenstates in the  $\text{X}^2\Sigma^+$  state, as the initial state  $|i\rangle$ , to one of the bound or unbound molecular eigenstates in the  $(5)^2\Sigma^+$  state, as the final state  $|f\rangle$ , with all the bound and unbound molecular eigenstates in the  $\text{A}^2\Pi$  state as the intermediate states

$|n\rangle$ 's. The simple three-level case corresponds to a single excitation channel having a single intermediate state. With the complete initial population at  $|i\rangle$ , the end amplitude  $A_f^{(i \rightarrow f)}$  and population  $P_f^{(i \rightarrow f)}$  of  $|f\rangle$  are given by the following frequency-domain expressions obtained within the framework of 2<sup>nd</sup>-order time-dependent perturbation theory [14, 21, 22]:

$$A_f^{(i \rightarrow f)} = \sum_n A_f^{(i \rightarrow n \rightarrow f)} = \sum_n \left\{ -\frac{1}{i\hbar^2} \mu_{fn} \mu_{ni} \left[ i\pi E(\omega_{ni}) E(\omega_{fi} - \omega_{ni}) \right. \right. \\ \left. \left. + \wp \int_{-\infty}^{\infty} \frac{1}{\omega_{ni} - \omega} E(\omega) E(\omega_{fi} - \omega) d\omega \right] \right\} \quad (1)$$

$$P_f^{(i \rightarrow f)} = \left| A_f^{(i \rightarrow f)} \right|^2, \quad (2)$$

where  $\sum_n$  stands for the summation over the intermediate discrete bound eigenstates and proper integral over the continuum unbound eigenstates, and  $\wp$  is the Cauchy's principal value. The  $\mu_{kl}$  and  $\omega_{kl} = (\mathcal{E}_k - \mathcal{E}_l)/\hbar$  are the full transition dipole moments (TDMs) and resonance frequency, respectively, between two eigenstates. The  $\mathcal{E}_i$  and  $\mathcal{E}_f$  are the energies of the initial and final states, respectively, while the  $\mathcal{E}_n$  is the energy of a given intermediate state  $n$ , with  $\omega_{fi} = \omega_{fn} + \omega_{ni}$ . The  $E(\omega) = |E(\omega)| \exp(-i\Phi(\omega))$  is the broad spectral field of the (linearly polarized) shaped femtosecond pulse, with  $|E(\omega)|$  and  $\Phi(\omega)$  being the spectral amplitude and phase, respectively. As seen, the amplitude  $A_f^{(i \rightarrow n \rightarrow f)}$  originating from excitation via a single intermediate state  $|n\rangle$  results from the interference among all the initial-to-final two-photon excitation pathways. Its first term includes the pathway on resonance with  $|n\rangle$ , while its second term incorporates all the near-resonant pathways.

Resulting from all the simultaneous excitation channels, the total population  $P_{\tilde{f} \in (5)^2\Sigma^+}$  of a given eigenstate  $|\tilde{f}\rangle$  in  $(5)^2\Sigma^+$  is the outcome of incoherent integral over contributions from all the different unbound eigenstates in  $\text{X}^2\Sigma^+$  according to their initial thermal population. So,

$$P_{\tilde{f} \in ((5)^2\Sigma^+, J_{5\Sigma}, M_{5\Sigma}, \nu_{5\Sigma}/\mathcal{E}_{5\Sigma})} = \frac{1}{\mathcal{Z}} \sum_{J_X, M_X} \\ \int_0^{\infty} d\mathcal{E}_X \rho(\mathcal{E}_X; J_X) \exp\left(-\frac{\mathcal{E}_X}{\kappa_B T}\right) P_{\tilde{f}}^{(\text{X}^2\Sigma^+, J_X, M_X, \mathcal{E}_X) \rightarrow \tilde{f}}, \quad (3)$$

where the unbound and bound eigenstates in a given electronic state are characterized here by their rotational quantum numbers  $J, M$  and, respectively, by their energy  $\mathcal{E}$  and/or vibrational quantum number  $\nu$ . The  $\mathcal{Z}$  is the

partition function,  $\rho(\mathcal{E}_X; J_X)$  is the density of unbound (continuum) states of  $X^2\Sigma^+$  at energy  $\mathcal{E}_X$  for a given  $J_X$ , and  $P_{\tilde{f}}^{(X^2\Sigma^+, J_X, M_X, \mathcal{E}_X) \rightarrow \tilde{f}}$  is described by Eqs. (1)-(2).

To reduce the computational effort, for a given  $|\tilde{f}\rangle$  in  $(5)^2\Sigma^+$ , the calculations include population contributions satisfying only  $J_X=J_{5\Sigma}$ , instead of all the transition-allowed possibilities of  $J_{5\Sigma}-J_X=0,\pm 1,\pm 2$ . For all the states  $|\tilde{f}\rangle$  that we have checked as examples, this change has only a minor effect on the calculated chirp dependence. The considered intermediate eigenstates in  $A^2\Pi$  are all the transition-allowed ones of  $J_A-J_{5\Sigma}=0,\pm 1$ . The calculated signal  $I_{5p}$  is taken as the total population of the  $(5)^2\Sigma^+$  state, i.e., summing all its eigenstates' populations.

As shown in Fig. 2, the theoretical results for the chirp dependence of  $I_{5p}$  reproduce the experimental ones to a very high degree, both qualitatively and quantitatively. Qualitatively, they exhibit all the experimental features of enhancement by negative chirps as well as the experimental trend of the general chirp dependence. The former includes the larger-than-1  $EF_{N/P}(|k|)$  values for all the chirp magnitudes, with a weak chirp dependence beyond small  $|k|$  values, and the larger-than-1  $EF(k)$  values for small negative chirps. Quantitatively, the theory-experiment fit for the EF results is excellent over the chirp range of  $-0.02$  to  $0.002$   $\text{ps}^2/\text{rad}$  and above  $0.02$   $\text{ps}^2/\text{rad}$ , including the corresponding maximal EF value of about 1.10, while at the other chirp values there is a small deviation of theory from experiment. This small deviation leads to calculated EF values that are slightly higher than the experimental ones. We assign that theoretical deviation in the EF values to the fact that the spin-orbit coupling is not included in our KAr model.

Following the theory-experiment agreement, we further theoretically analyze the system to identify the chirp control mechanism. A corresponding insight can be found by comparing the spectral locations of the two excitation FCWs. As mentioned and seen in Fig. 1, for the  $X^2\Sigma^+ - A^2\Pi$  FCW it is the full pulse spectrum, while for the  $A^2\Pi - (5)^2\Sigma^+$  FCW it is only the low-frequency edge of the spectrum. Hence, most of the  $(5)^2\Sigma^+$ 's population is excited via initial-to-final excitation channels with intermediate eigenstates, for which the initial-to-intermediate transition frequency ( $\omega_{ni}$ ) is higher than the intermediate-to-final one ( $\omega_{fn}$ ), i.e.,  $\omega_{ni} > \omega_{fn}$ . For a given excitation channel, these dominant intermediate eigenstates are those that are energetically connected by the pulse spectrum to both the initial and final eigenstates and, simultaneously, also have large-enough VTDMs with them both. For a weak-field resonance-mediated two-photo absorption in a bound three-level (initial-intermediate-final) system, it has previously been shown [21, 22] that an enhancement by negative chirps exists when  $\omega_{ni} > \omega_{fn}$ . From a time-domain point of view,

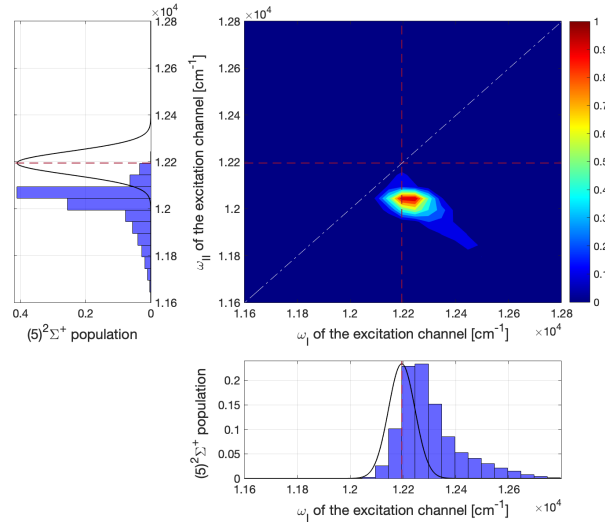


FIG. 3: Theoretical results for the effect of the two-step Franck-Condon filtering. All the  $(5)^2\Sigma^+$  population is excited via channels having their averaged first transition frequency ( $\omega_I$ ) higher than their second one ( $\omega_{II}$ ). The plotted results are for the TL pulse excitation. The map shows the  $(5)^2\Sigma^+$  population integrated over all the excitation channels that are characterized by given values for  $\omega_I$  and  $\omega_{II}$ . The line of equality between the two frequencies is indicated by a white dashed line. The map projections on the two frequency axes are shown as histograms, each plotted on top of the pulse spectrum. See text for details.

the negatively-chirped pulses photo-induce an optimal excitation sequence: the temporally-decreasing instantaneous pulse frequency comes into resonance first with  $\omega_{ni}$  and only then with  $\omega_{fn}$ . From a frequency-domain point of view, the negative chirps enhance the degree of constructive interferences, over destructive ones, among the two-photon excitation pathways. Hence, we identify the present control mechanism to be the combination of (i) extended Franck-Condon filtering [6, 7] incorporating two steps, which purifies the full thermal ensemble of excitation channels and filter out a sub-ensemble of channels that is susceptible for chirp control, and (ii) chirp-dependent resonance-mediated excitation of the filtered sub-ensemble. The present enhancement by negative chirps is explained by the fact that the filtered sub-ensemble of excitation channels is characterized by effective transition frequencies for which negative chirps are optimal. The control power of a negatively chirped pulse lies here also in the fact that it can simultaneously act in an optimal way over a multitude of excitation channels and intermediate states with many different individual transition frequencies  $\omega_{ni}$  and  $\omega_{fn}$ , as long as the relation  $\omega_{ni} > \omega_{fn}$  is satisfied for all of them.

To quantitatively analyze our system along this line, we apply the following statistical analysis. Each of the two steps of a given initial-to-final excitation channel is characterized by an effective transition fre-

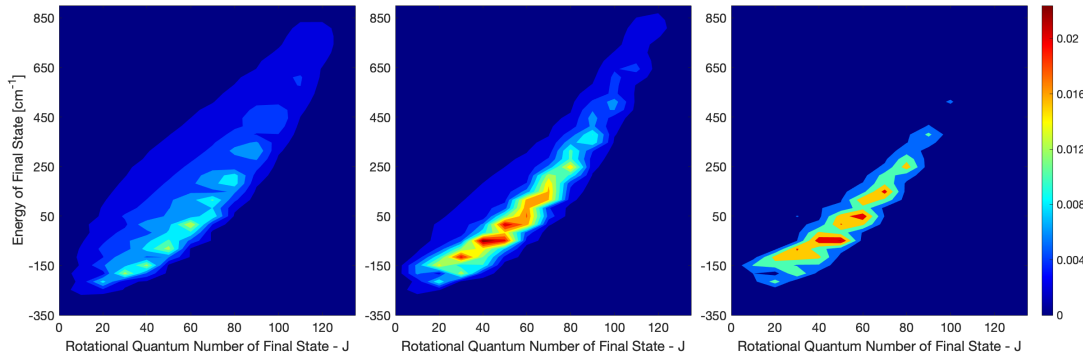


FIG. 4: Theoretical results for coherent control over the final population distribution. The distribution of the relative population of the different final eigenstates in the  $(5)^2\Sigma^+$  state is shown for excitations by the TL pulse (left panel) and linearly-chirped pulses of chirps  $-0.01$  (middle panel) and  $-0.02$  rad/ps $^2$  (right panel). The relative population is shown as a function of the rotational quantum number and energy of the final eigenstate. Each distribution is normalized to a population sum of 1.

quency,  $\omega_I^{(i \rightarrow f)}$  and  $\omega_{II}^{(i \rightarrow f)}$ , calculated as a corresponding weighted average over all the intermediate eigenstates as  $\omega_I^{(i \rightarrow f)} = \sum_n \omega_{ni} P_{f;TL}^{(i \rightarrow n \rightarrow f)}$  and  $\omega_{II}^{(i \rightarrow f)} = \sum_n \omega_{fn} P_{f;TL}^{(i \rightarrow n \rightarrow f)}$  with  $P_{f;TL}^{(i \rightarrow n \rightarrow f)} = |A_{f;TL}^{(i \rightarrow n \rightarrow f)}|^2$  [see Eq. (1)] where  $\{i \in X^2\Sigma^+, n \in A^2\Pi, f \in (5)^2\Sigma^+\}$ . The population  $P_{f;TL}^{(i \rightarrow n \rightarrow f)}$  corresponds to the excited population in the isolated  $i$ - $n$ - $f$  system with the TL pulse. Then, a map representing the full ensemble of excitation channels is generated, showing the sum over all the populations  $P_{f;TL}^{(i \rightarrow f)}$  excited via channels that are characterized by given values of  $\omega_I^{(i \rightarrow f)}$  and  $\omega_{II}^{(i \rightarrow f)}$ . Figure 3 shows this calculated map, together with the corresponding histograms resulting from the projections on each of its axes. The bin width of the histograms is 50 cm $^{-1}$ . It is comparable to the average value of the weighted standard deviation of the different transition frequencies corresponding to the different intermediates within a single excitation channel. As the results show, more than 99% of the total  $(5)^2\Sigma^+$ 's population is excited via channels that are characterized by  $\omega_I^{(i \rightarrow f)} > \omega_{II}^{(i \rightarrow f)}$ . For both histograms, the frequency values corresponding to most of the histogram's population indeed fits the spectral position of the corresponding FCW. So, it is confirmed that the described two-step Franck-Condon filtering (TS-FCF) is indeed active here and, following its action, the enhancement by negative chirps is indeed expected.

The critical role of the TS-FCF for the chirp control is also illustrated by the theoretical results obtained with artificially setting all the system's VTDMs to the same value, ignoring their true values. This corresponds to eliminating the TS-FCF mechanism, such that the system excitation (under the rotational selection rules) is affected only by the state energies and pulse spectrum. As shown in Fig. 2 (solid gray lines), indeed, without the TS-FCF, the enhancement by negative chirps is almost completely gone: the maximal signal is obtained for the TL pulse, i.e., there is no enhancement of negatively

chirped pulses over the TL pulse, and the  $E_{NP}$  values are all around 1 for all the chirp magnitudes.

Another important control insight obtained from the calculations (with TS-FCF) is that the degree of enhancement by negative chirps, obtained for the present system with a given pulse spectrum, increases as the number of dominant intermediate eigenstates within a single excitation channel decreases (and, correspondingly, decreases as the number increases). This number can be quantitatively considered, for example, as the minimal number of intermediates that cumulatively contribute more than 90% of the channel's excited population. The effect is clearly shown in Fig. 2 by the chirp-dependent theoretical results obtained for  $I_{5p}$  in the two cases of including either only bound or only unbound eigenstates in  $A^2\Pi$  as the excitation's intermediates. The average number of dominant intermediates within a channel is naturally much higher when considering only unbound intermediates (which are part of the continuum) as compared to considering only bound ones. As seen in the figure, the degree of enhancement by negative chirps is much higher in the bound case as compared to the unbound one, both in terms of the  $EF$  values at all the negative chirps, including the maximal  $EF$ , and of the  $EF_{N/P}$  values at all the chirp magnitudes. The effect results from the coherent interferences among the different final-state amplitudes that are excited via the different intermediate states ( $A_f^{(i \rightarrow n \rightarrow f)}$ ). For an excitation with a chirped pulse, each of these amplitudes generally has a different phase, hence summing up more amplitudes further diminishes the control degree. As also seen, the corresponding results for the real case of the experiment and theory, i.e., when both the bound and unbound eigenstates in  $A^2\Pi$  are the intermediates, fall in between these two individual cases. It also worth mentioning that the absolute  $(5)^2\Sigma^+$ 's populations calculated in the separate bound and unbound cases for the TL pulse are comparable, with a corresponding ratio of about 0.45:0.55, re-

spectively.

Last, we theoretically analyze the final population distribution and its chirp control. Figure 4 shows the corresponding results. The distribution of the relative population of the different final eigenstates in the  $(5)^2\Sigma^+$  state is shown for excitations by the TL pulse and linearly-chirped pulses of chirps  $-0.01$  and  $-0.02$  rad/ps $^2$ . The relative population is presented as a function of the rotational quantum number  $J_{5\Sigma}$  and energy  $\mathcal{E}_{5\Sigma}$  of the final eigenstate. Each distribution is normalized to a population sum of 1. In terms of the general characteristics of the distribution, the following is observed. The present excitation involves high rotations of up to  $J_{5\Sigma} \sim 100-130$ , with the maximal population being excited at  $J_{5\Sigma} \sim 40-60$  at all the chirp cases. For all the pulses, the excited population shows a clear correlation between  $J_{5\Sigma}$  and  $\mathcal{E}_{5\Sigma}$ , where, for a given  $J_{5\Sigma}$ , there is only a selective band of energies  $\mathcal{E}_{5\Sigma}$  that gets populated. The higher the rotation, the higher is the energetic location of the band. This correlation originates from the first step of the TS-FCF, where for a given initial rotation  $J_X$  there is only a band of initial collision energies  $\mathcal{E}_X$  that allows the collision pair to properly reach the X-A FCW at the short internuclear distances. Only at these collision energies, the scattering state's wavefunction has large enough non-oscillatory amplitude within the X-A FCW. This rotational-translational correlation existing for the initial eigenstates of the dominant excitation channels directly leads to a similar correlation for their final eigenstates. It is so since, from a given initial energy  $\mathcal{E}_X$ , there is only a limited range of final energies  $\mathcal{E}_{5\Sigma}$  that are effectively accessible by the weak-field two-photon excitation with a given pulse spectrum, and the location of this final range increases as  $\mathcal{E}_X$  increases. In terms of the control, as seen, there is a clear and prominent chirp dependence of the generated relative population distribution for negative chirps - as the negative chirp magnitude increases from zero chirp, the distribution gets narrower and narrower in terms of both  $J_{5\Sigma}$  and  $\mathcal{E}_{5\Sigma}$ . For all the present positive chirps, the distribution (not shown here) is almost chirp independent and stays very close to the one generated by the TL pulse.

In summary, we extend femtosecond coherent control of thermally-hot unbound collision pair to the important weak-field regime both in experiment and theory. The work is also the first to demonstrate weak-field femtosecond control of an initially-unbound system. Linearly chirped pulses coherently control the photo-excitation yield of an ensemble of unbound collision pairs, which are excited at short internuclear distances from their scattering states via a thermal molecular resonance-mediated two-photon absorption process. Enhancement by negatively chirped pulses is observed relative to the positively chirped pulses of the same linear chirp magnitude as well as relative to the TL pulse. Our first-principles theoretical modeling has allowed us to identify the co-

herent control mechanism as the combination of two-step Franck-Condon filtering and chirp-dependent resonance-mediated excitation of the filtered excitation channels. The former purifies the extended thermal ensemble of excitation channels and filters out a sub-ensemble of channels that is susceptible for chirp control, while the latter realizes the (phase) control over the selected sub-ensemble by utilizing chirp-dependent coherent interferences. The theoretical results also show that a prominent control is obtained over the final population distribution. Weak-field femtosecond coherent control strategy and tools are now added to the control toolbox of a thermal unbound collision pair, establishing another milestone toward coherent control of photoinduced binary reactions.

Financial support from the Deutsche Forschungsgemeinschaft (DFG—German Research Foundation) under the DFG Priority Program 1840, ‘Quantum Dynamics in Tailored Intense Fields (QUTIF)’, is gratefully acknowledged.

---

\* E-mail: amitayz@technion.ac.il

- [1] D. J. Tannor and S. A. Rice, *The Journal of Chemical Physics* **83**, 5013 (1985).
- [2] R. Kosloff, S. A. Rice, P. Gaspard, S. Tersigni, and D. Tannor, *Chemical Physics* **139**, 201 (1989).
- [3] S. A. Rice and M. Zhao, *Optical control of molecular dynamics* (John Wiley & Sons, 2000).
- [4] M. Shapiro and P. Brumer, *Principles of the quantum control of molecular processes* (Wiley Interscience, 2003).
- [5] A. M. Weiner, *Review of scientific instruments* **71**, 1929 (2000).
- [6] L. Rybak, S. Amaran, L. Levin, M. Tomza, R. Moszynski, R. Kosloff, C. P. Koch, and Z. Amitay, *Physical Review Letters* **107**, 273001 (2011).
- [7] S. Amaran, R. Kosloff, M. Tomza, W. Skomorowski, F. Pawłowski, R. Moszynski, L. Rybak, L. Levin, Z. Amitay, J. M. Berglund, et al., *The Journal of Chemical Physics* **139**, 164124 (2013).
- [8] L. Levin, W. Skomorowski, L. Rybak, R. Kosloff, C. P. Koch, and Z. Amitay, *Physical Review Letters* **114**, 233003 (2015).
- [9] L. Levin, W. Skomorowski, R. Kosloff, C. P. Koch, and Z. Amitay, *Journal of Physics B: Atomic, Molecular and Optical Physics* **48**, 184004 (2015).
- [10] L. Levin, D. M. Reich, M. Geva, R. Kosloff, C. P. Koch, and Z. Amitay, *Journal of Physics B: Atomic, Molecular and Optical Physics* **54**, 144007 (2021).
- [11] D. Meshulach and Y. Silberberg, *Nature* **396**, 239 (1998).
- [12] D. Meshulach and Y. Silberberg, *Phys. Rev. A* **60**, 1287 (1999).
- [13] S. Zamith, J. Degert, S. Stock, B. de Beauvoir, V. Blanchet, M. Aziz Bouchene, and B. Girard, *Phys. Rev. Lett.* **87**, 033001 (2001).
- [14] N. Dudovich, B. Dayan, S. M. Gallagher Faeder, and Y. Silberberg, *Phys. Rev. Lett.* **86**, 47 (2001).
- [15] H. U. Stauffer, J. B. Ballard, Z. Amitay, and S. R. Leone, *The Journal of Chemical Physics* **116**, 946 (2002).

- [16] N. Dudovich, D. Oron, and Y. Silberberg, Phys. Rev. Lett. **88**, 123004 (2002).
- [17] N. Dudovich, D. Oron, and Y. Silberberg, Nature **418**, 512 (2002).
- [18] J. Degert, W. Wohlleben, B. Chatel, M. Motzkus, and B. Girard, Phys. Rev. Lett. **89**, 203003 (2002).
- [19] D. Oron, N. Dudovich, and Y. Silberberg, Phys. Rev. Lett. **89**, 273001 (2002).
- [20] V. V. Lozovoy, I. Pastirk, K. A. Walowicz, and M. Dan-tus, The Journal of Chemical Physics **118**, 3187 (2003).
- [21] B. Chatel, J. Degert, S. Stock, and B. Girard, Phys. Rev. A **68**, 041402 (2003).
- [22] B. Chatel, J. Degert, and B. Girard, Phys. Rev. A **70**, 053414 (2004).
- [23] N. Dudovich, D. Oron, and Y. Silberberg, Phys. Rev. Lett. **92**, 103003 (2004).
- [24] A. Prakelt, M. Wollenhaupt, C. Sarpe-Tudoran, and T. Baumert, Phys. Rev. A **70**, 063407 (2004).
- [25] X. Dai, E.-B. W. Lerch, and S. R. Leone, Phys. Rev. A **73**, 023404 (2006).
- [26] S.-H. Lim, A. G. Caster, and S. R. Leone, Phys. Rev. A **72**, 041803 (2005).
- [27] A. Gandman, L. Chuntonov, L. Rybak, and Z. Amitay, Phys. Rev. A **75**, 031401 (2007).
- [28] A. Gandman, L. Chuntonov, L. Rybak, and Z. Amitay, Phys. Rev. A **76**, 053419 (2007).
- [29] Z. Amitay, A. Gandman, L. Chuntonov, and L. Rybak, Phys. Rev. Lett. **100**, 193002 (2008).
- [30] A. Gandman, L. Rybak, and Z. Amitay, Phys. Rev. Lett. **113**, 043003 (2014).
- [31] D. L. Thompson, The Journal of Chemical Physics **76**, 1806 (1982).
- [32] R. Berends, W. Kedzierski, J. Atkinson, and L. Krause, Spectrochimica Acta Part B: Atomic Spectroscopy **43**, 1069 (1988).
- [33] A. Mills, J. A. Behr, L. A. Courneyea, and M. R. Pearson, Phys. Rev. A **72**, 024501 (2005).
- [34] U. I. Safronova and M. S. Safronova, Phys. Rev. A **78**, 052504 (2008).
- [35] E. Epifanovsky, A. T. B. Gilbert, X. Feng, J. Lee, Y. Mao, N. Mardirossian, P. Pokhilko, A. F. White, M. P. Coons, A. L. Dempwolff, et al., The Journal of Chemical Physics **155**, 084801 (2021).
- [36] M. B. E. H. Rhouma, H. Berriche, Z. B. Lakhdar, and F. Spiegelman, The Journal of Chemical Physics **116**, 1839 (2002).
- [37] L. Blank, D. E. Weeks, and G. S. Kedziora, The Journal of Chemical Physics **136**, 124315 (2012).